Observation of $b \to d\gamma$ and Determination of $|V_{td}/V_{ts}|$

D. Mohapatra,[48] M. Nakao,[6] S. Nishida,[6] K. Abe,[6] K. Abe,[41] I. Adachi,[6] H. Aihara,[43] D. Anipko,[1] K. Arinstein,[1] Y. Asano,[47] V. Aulchenko,[1] T. Aushev,[10] S. Bahinipati,[3] A. M. Bakich,[38] V. Balagura,[10] M. Barbero,[5] I. Bedny,[1] U. Bitenc,[11] I. Bizjak,[11] S. Blyth,[21] A. Bondar,[1] A. Bozek,[24] M. Bračko,[6,17,11] T. E. Browder,[5] Y. Chao,[23] A. Chen,[21] K.-F. Chen,[23] W. T. Chen,[21] B. G. Cheon,[2] R. Chistov,[10] Y. Choi,[37] A. Chuvikov,[32] S. Cole,[38] J. Dalseno,[18] M. Danilov,[10] M. Dash,[48] J. Dragic,[6] A. Drutskoy,[3] S. Eidelman,[1] D. Epifanov,[1] S. Fratina,[11] N. Gabyshev,[1] T. Gershon,[6] G. Gokhroo,[39] B. Golob,[16,11] A. Gorišek,[11] H. C. Ha,[13] J. Haba,[6] T. Hara,[29] N. C. Hastings,[43] K. Hayasaka,[19] H. Hayashii,[20] M. Hazumi,[6] L. Hinz,[15] T. Hokuue,[19] Y. Hoshi,[41] S. Hou,[21] W.-S. Hou,[23] Y. B. Hsiung,[23] T. Iijima,[19] A. Imoto,[20] K. Inami,[19] A. Ishikawa,[6] H. Ishino,[44] R. Itoh,[6] M. Iwasaki,[43] Y. Iwasaki,[6] J. H. Kang,[49] S. U. Kataoka,[20] N. Katayama,[6] T. Kawasaki,[26] H. R. Khan,[44] H. Kichimi,[6] H. J. Kim,[14] H. O. Kim,[37] S. M. Kim,[37] K. Kinoshita,[3] S. Korpar,[17,11] P. Križan,[16,11] P. Krokovny,[1] R. Kulasiri,[3] R. Kumar,[30] C. C. Kuo,[21] A. Kuzmin,[1] Y.-J. Kwon,[49] J. S. Lange,[4] G. Leder,[8] J. Lee,[36] T. Lesiak,[24] A. Limosani,[6] S.-W. Lin,[23] D. Liventsev,[10] G. Majumder,[39] F. Mandl,[8] D. Marlow,[32] T. Matsumoto,[45] A. Matyja,[24] W. Mitaroff,[8] K. Miyabayashi,[20] H. Miyake,[29] H. Miyata,[26] Y. Miyazaki,[19] R. Mizuk,[10] G. R. Moloney,[18] T. Mori,[44] E. Nakano,[28] O. Nitoh,[46] T. Nozaki,[6] S. Ogawa,[40] T. Ohshima,[19] T. Okabe,[19] S. Okuno,[12] S. L. Olsen,[5] H. Ozaki,[6] P. Pakhlov,[10] H. Palka,[24] C. W. Park,[37] N. Parslow,[38] L. S. Peak,[38] R. Pestotnik,[11] L. E. Piilonen,[48] A. Poluektov,[1] F. J. Ronga,[6] M. Rozanska,[24] Y. Sakai,[6] T. R. Sarangi,[6] N. Sato,[19] T. Schietinger,[15] O. Schneider,[15] J. Schümann,[23] C. Schwanda,[8] A. J. Schwartz,[3] R. Seidl,[33] M. E. Sevior,[18] M. Shapkin,[9] H. Shibuya,[40] B. Shwartz,[1] V. Sidorov,[1] A. Sokolov,[9] A. Somov,[3] N. Soni,[30] R. Stamen,[6] S. Stanič,[27] M. Starič,[11] T. Sumiyoshi,[45] S. Suzuki,[34] O. Tajima,[6] F. Takasaki,[6] K. Tamai,[6] N. Tamura,[26] M. Tanaka,[6] G. N. Taylor,[18] Y. Teramoto,[28] X. C. Tian,[31] K. Trabelsi,[5] T. Tsukamoto,[6] S. Uehara,[6] T. Uglov,[10] K. Ueno,[23] Y. Unno,[6] S. Uno,[6] P. Urquijo,[18] Y. Usov,[1] G. Varner,[5] K. E. Varvell,[38] S. Villa,[15] C. C. Wang,[23] C. H. Wang,[22] M.-Z. Wang,[23] Y. Watanabe,[44] J. Wicht,[15] E. Won,[13] Q. L. Xie,[7] B. D. Yabsley,[38] A. Yamaguchi,[42] Y. Yamashita,[25] M. Yamauchi,[6] J. Ying,[31] Y. Yusa,[42] L. M. Zhang,[35] Z. P. Zhang,[35] V. Zhilich,[1] and D. Zürcher[15]

(Belle Collaboration)

[1]*Budker Institute of Nuclear Physics, Novosibirsk*
[2]*Chonnam National University, Kwangju*
[3]*University of Cincinnati, Cincinnati, Ohio 45221*
[4]*University of Frankfurt, Frankfurt*
[5]*University of Hawaii, Honolulu, Hawaii 96822*
[6]*High Energy Accelerator Research Organization (KEK), Tsukuba*
[7]*Institute of High Energy Physics, Chinese Academy of Sciences, Beijing*
[8]*Institute of High Energy Physics, Vienna*
[9]*Institute of High Energy Physics, Protvino*
[10]*Institute for Theoretical and Experimental Physics, Moscow*
[11]*J. Stefan Institute, Ljubljana*
[12]*Kanagawa University, Yokohama*
[13]*Korea University, Seoul*
[14]*Kyungpook National University, Taegu*
[15]*Swiss Federal Institute of Technology of Lausanne, EPFL, Lausanne*
[16]*University of Ljubljana, Ljubljana*
[17]*University of Maribor, Maribor*
[18]*University of Melbourne, Victoria*
[19]*Nagoya University, Nagoya*
[20]*Nara Women's University, Nara*
[21]*National Central University, Chung-li*
[22]*National United University, Miao Li*
[23]*Department of Physics, National Taiwan University, Taipei*
[24]*H. Niewodniczanski Institute of Nuclear Physics, Krakow*
[25]*Nippon Dental University, Niigata*
[26]*Niigata University, Niigata*
[27]*Nova Gorica Polytechnic, Nova Gorica*
[28]*Osaka City University, Osaka*

[29]Osaka University, Osaka
[30]Panjab University, Chandigarh
[31]Peking University, Beijing
[32]Princeton University, Princeton, New Jersey 08544
[33]RIKEN BNL Research Center, Upton, New York 11973
[34]Saga University, Saga
[35]University of Science and Technology of China, Hefei
[36]Seoul National University, Seoul
[37]Sungkyunkwan University, Suwon
[38]University of Sydney, Sydney NSW
[39]Tata Institute of Fundamental Research, Bombay
[40]Toho University, Funabashi
[41]Tohoku Gakuin University, Tagajo
[42]Tohoku University, Sendai
[43]Department of Physics, University of Tokyo, Tokyo
[44]Tokyo Institute of Technology, Tokyo
[45]Tokyo Metropolitan University, Tokyo
[46]Tokyo University of Agriculture and Technology, Tokyo
[47]University of Tsukuba, Tsukuba
[48]Virginia Polytechnic Institute and State University, Blacksburg, Virginia 24061
[49]Yonsei University, Seoul

(Received 13 February 2006; published 9 June 2006)

We report the observation of the flavor-changing neutral current process $b \to d\gamma$ using a sample of 386×10^6 B meson pairs accumulated by the Belle detector at the KEKB e^+e^- collider. We measure branching fractions for the exclusive modes $B^- \to \rho^-\gamma$, $\bar{B}^0 \to \rho^0\gamma$, and $\bar{B}^0 \to \omega\gamma$. Assuming that these three modes are related by isospin, we find $\mathcal{B}(\bar{B} \to (\rho, \omega)\gamma) = (1.32^{+0.34}_{-0.31}(\text{stat})^{+0.10}_{-0.09}(\text{syst})) \times 10^{-6}$ with a significance of 5.1σ. This result is used to determine the ratio of Cabibbo-Kobayashi-Maskawa matrix elements $|V_{td}/V_{ts}|$ to be $0.199^{+0.026}_{-0.025}(\text{exp})^{+0.018}_{-0.015}(\text{theor})$.

DOI: 10.1103/PhysRevLett.96.221601 PACS numbers: 13.20.He, 12.15.Hh, 12.15.Mm, 14.40.Nd

The $b \to d\gamma$ process, which proceeds via a loop diagram [Fig. 1(a)] in the standard model (SM), is suppressed with respect to $b \to s\gamma$ by the Cabibbo-Kobayashi-Maskawa (CKM) factor [1] $|V_{td}/V_{ts}|^2 \sim 0.04$, with large uncertainty due to the lack of precise knowledge of $|V_{td}|$. The exclusive modes $\bar{B} \to \rho\gamma$ and $\bar{B}^0 \to \omega\gamma$ are presumably the easiest modes to search for; no evidence for the decays has been previously reported [2,3]. The predicted branching fractions are $(0.9\text{–}2.7) \times 10^{-6}$ [4,5] based on the measured rate for the $b \to s\gamma$ process $\bar{B} \to \bar{K}^*\gamma$ and the $|V_{td}/V_{ts}|^2$ factor with corrections due to form factors, $SU(3)$ breaking effects, and, for the B^- decay, inclusion of an annihilation diagram [Fig. 1(b)]. Measurement of these exclusive branching fractions allows one to determine the value of $|V_{td}/V_{ts}|$ in the context of the SM and to search for physics beyond the SM [6]. In this Letter, we report the observation of the $b \to d\gamma$ process using a sample of $(386 \pm 5) \times 10^6$ B meson pairs accumulated at the $\Upsilon(4S)$ resonance. With a larger data sample and an improved analysis procedure, the results supersede those of our previous publication [2].

The data are produced in e^+e^- annihilation at the KEKB energy-asymmetric (3.5 on 8 GeV) collider [7] and collected with the Belle detector [8], which includes a silicon vertex detector (SVD), a central drift chamber (CDC), aerogel threshold Cherenkov counters (ACC), time-of-flight (TOF) scintillation counters, and an electromagnetic calorimeter (ECL) of CsI(Tl) crystals located inside a 1.5 T superconducting solenoid coil.

We reconstruct three signal modes, $B^- \to \rho^-\gamma$, $\bar{B}^0 \to \rho^0\gamma$, and $\bar{B}^0 \to \omega\gamma$, and two control samples, $B^- \to K^{*-}\gamma$ and $\bar{B}^0 \to \bar{K}^{0*}\gamma$. Charge conjugate modes are implicitly included throughout this Letter. The following decay modes are used to reconstruct the intermediate states: $\rho^- \to \pi^-\pi^0$, $\rho^0 \to \pi^+\pi^-$, $\omega \to \pi^+\pi^-\pi^0$, $K^{*-} \to K^-\pi^0$, $\bar{K}^{*0} \to K^-\pi^+$, and $\pi^0 \to \gamma\gamma$.

Photon candidates are reconstructed from ECL energy clusters with a photonlike shape and no associated charged track. A photon in the barrel ECL ($33° < \theta_\gamma < 128°$ in the laboratory frame polar angle) with a center-of-mass (c.m.) energy in the range $1.8\ \text{GeV} < E_\gamma < 3.4\ \text{GeV}$ is selected as the primary photon candidate. To suppress backgrounds from $\pi^0/\eta \to \gamma\gamma$ decays, we apply a veto algorithm based on likelihoods to be and not to be a π^0/η. The likelihoods are calculated for every combination of the primary photon

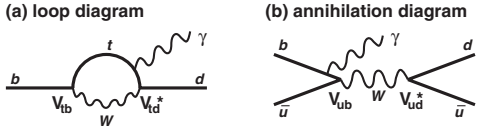

FIG. 1. (a) Loop diagram for $b \to d\gamma$ and (b) annihilation diagram, which contributes only to $B^- \to \rho^-\gamma$.

and another photon in the event using the energy of the other photon and the invariant mass of the pair. We also reject the primary photon candidate if the ratio of the energy in the central 3×3 ECL cells to that in the central 5×5 cells is less than 0.95.

Neutral pions are formed from photon pairs with invariant masses within ± 16 MeV/c^2 ($\sim 3\sigma$) of the π^0 mass. The photon momenta are then recalculated with a π^0 mass constraint. We require the energy of each photon to be greater than 50 (100) MeV inside (outside) the barrel ECL. We also require the cosine of the angle between the two photons in the laboratory frame to be greater than 0.7; this requirement suppresses the copious combinatorial background with momenta below 0.6 GeV/c.

Charged pions and kaons are selected from tracks in the CDC and SVD. Each track is required to have a transverse momentum greater than 100 MeV/c and a distance of closest approach to the interaction point of less than 0.5 cm in radius and ± 3.0 cm along the z axis, which is parallel to the positron beam. We do not use a track to form the signal candidate if, when it is combined with an oppositely charged track, the resulting pair has an invariant mass within ± 30 MeV/c^2 of the K^0_S mass and a displaced vertex that is consistent with that of a K^0_S. We determine pion ($\mathcal{L}_\pi$) and kaon ($\mathcal{L}_K$) likelihoods from ACC, CDC, and TOF information and form a likelihood ratio $\mathcal{L}_\pi/(\mathcal{L}_\pi + \mathcal{L}_K)$ to separate pions from kaons. The criteria for pions have efficiencies of 83%, 81%, and 91% for ρ^-, ρ^0, and ω, respectively; the corresponding kaon misidentification rates are 5.8%, 6.3%, and 8.4%. For K^* candidates, we select kaons with an efficiency of 90%.

Invariant masses for the ρ, ω, and K^* candidates are required to be within windows of ± 150, ± 30, and ± 75 MeV/c^2, respectively, around their nominal values.

Candidate B mesons are reconstructed by combining a ρ or ω candidate with the primary photon and calculating two variables: the beam-energy constrained mass $M_{\rm bc} = \sqrt{(E^*_{\rm beam}/c^2)^2 - |\vec{p}^{\,*}_B/c|^2}$, and the energy difference $\Delta E = E^*_B - E^*_{\rm beam}$. Here, $\vec{p}^{\,*}_B$ and E^*_B are the c.m. momentum and energy of the B candidate, and $E^*_{\rm beam}$ is the c.m. beam energy. To improve resolution, the magnitude of the photon momentum is replaced by $(E^*_{\rm beam} - E^*_{\rho/\omega})/c$ when the momentum $\vec{p}^{\,*}_B$ is calculated.

To optimize the event selection, we study Monte Carlo (MC) events in a signal box defined as $5.273\ {\rm GeV}/c^2 < M_{\rm bc} < 5.285\ {\rm GeV}/c^2$ and $-0.10\,{\rm GeV} < \Delta E < 0.08\,{\rm GeV}$. We choose selection criteria to maximize $N_S/\sqrt{N_B}$, where N_S and N_B are the expected signal and the sum of the background yields.

The dominant background arises from continuum events [$e^+e^- \to q\bar{q}(\gamma)$, $q = u, d, s, c$], where a random combination of a ρ or ω candidate with a photon forms a B candidate. We suppress this background using the following quantities: (1) $\mathcal{F}$, a Fisher discriminant constructed from 16 modified Fox-Wolfram moments [9,10] and the scalar sum of the transverse momenta of all charged tracks and photons. (2) $\cos\theta^*_B$, where θ^*_B is the c.m. polar angle of the B candidate direction: true B mesons follow a $1 - \cos^2\theta^*_B$ distribution, while candidates in the continuum background are almost uniformly distributed. (3) Δz, the separation along the z axis between the decay vertex of the candidate B meson and the fitted vertex of the remaining tracks in the event. Discrimination is provided due to the displacement of the signal B decay vertex from the other B, as tracks from continuum events typically have a common vertex. For each of the quantities $\mathcal{F}$, $\cos\theta^*_B$, and Δz, we construct likelihood distributions for signal and continuum events. The $\mathcal{F}$, $\cos\theta^*_B$, and signal Δz distributions are determined from MC samples; the continuum Δz distribution is determined from the data sideband $5.20\ {\rm GeV}/c^2 < M_{\rm bc} < 5.24\ {\rm GeV}/c^2$, $-0.1\ {\rm GeV} < \Delta E < 0.5\ {\rm GeV}$.

We form product likelihoods $\mathcal{L}_s$ and $\mathcal{L}_c$ for signal and continuum background, respectively, from the likelihood distributions for $\mathcal{F}$, $\cos\theta^*_B$, and (where available) Δz. In addition, we use a tagging quality variable r that indicates the level of confidence in the B-flavor determination as described in Ref. [11]. In the $(r, \mathcal{R})$ plane defined by the tagging quality r and the likelihood ratio $\mathcal{R} = \mathcal{L}_s/(\mathcal{L}_s + \mathcal{L}_c)$, signal tends to populate the edges at $r = 1$ and $\mathcal{R} = 1$, while continuum preferentially populates the edges at $r = 0$ and $\mathcal{R} = 0$. We divide the events into six bins of r (two bins between 0 and 0.5, and four between 0.5 and 1) and determine the minimum $\mathcal{R}$ requirement for each bin. In the $\rho^-\gamma$ mode, we also assign events to the bin $0 \le r < 0.25$ if the tagging-side flavor is the same as the signal side. The signal efficiency is $\sim 40\%$, and $\sim 95\%$ of continuum background is rejected. For the $K^{*-}\gamma$ ($\bar{K}^{*0}\gamma$) mode we use the selection criteria for the $\rho^-\gamma$ ($\rho^0\gamma$) mode.

We consider the following backgrounds from B decays: $\bar{B} \to \bar{K}^*\gamma$, other $B \to X_s\gamma$ processes, decays with a π^0/η ($B \to \rho\pi^0$, $\omega\pi^0$, $\rho\eta$, and $\omega\eta$), other charmless hadronic B decays, and $b \to c$ decay modes. We find the $b \to c$ background to be negligible. The $\bar{B} \to \bar{K}^*\gamma$ background can mimic the $\overline{B} \to \rho\gamma$ signal if the kaon from the K^* is misidentified as a pion. To suppress $\bar{B} \to \bar{K}^*\gamma$ events we calculate $M_{K\pi}$, where the kaon mass is assigned to one of the charged pion candidates, and reject the candidate if $M_{K\pi} < 0.95(0.92)\ {\rm GeV}/c^2$ for the $\rho^0\gamma$ ($\rho^-\gamma$) mode. This requirement removes 82% (64%) of the $K^*\gamma$ background while retaining 63% (87%) of the signal. The decay chain $\bar{B}^0 \to \bar{K}^{*0}\gamma$, $\bar{K}^{*0} \to K^0_S\pi^0$, $K^0_S \to \pi^+\pi^-$ has a small contribution to $\bar{B}^0 \to \omega\gamma$ due to the tail of the K^* Breit-Wigner line shape. In addition, $\bar{B} \to \bar{K}^*\gamma$ and other $B \to X_s\gamma$ decays contribute to the background when the ρ and ω candidates are formed from random combinations of particles.

Hadronic decays with a π^0/η can mimic the signal if a photon from the π^0 or $\eta \to \gamma\gamma$ decay is soft and passes the π^0/η veto. To suppress this background, we reject the candidate if $|\cos\theta_{\rm hel}| > 0.75$, 0.70, and 0.80 for the $\rho^-\gamma$,

$\rho^0\gamma$, and $\omega\gamma$ modes, respectively, where the helicity angle $\theta_{\rm hel}$ is the angle between the π^- track (normal to the ω decay plane) and the B momentum vector in the ρ (ω) rest frame (similarly for the $K^*\gamma$ modes). Other hadronic decays make smaller contributions.

The reconstruction efficiency for each mode is defined as the fraction of the signal remaining after all selection criteria are applied, where the signal yield is determined from a fit to the sum of the signal and continuum MC samples using the procedure described below. The total efficiencies are listed in Table I. The systematic error on the efficiency is the quadratic sum of the following contributions, estimated using control samples: the uncertainty in the photon detection efficiency (2.2%) as measured in radiative Bhabha events; charged tracking efficiency (1.0% per track) from partially reconstructed $D^{*+} \to D^0\pi^+$, $D^0 \to K^0_S\pi^+\pi^-$, $K^0_S \to \pi^+(\pi^-)$; charged pion and kaon identification (0.7%–1.7% per track) and misidentification (15%–17%) from $D^{*+} \to D^0\pi^+$, $D^0 \to K^-\pi^+$; neutral pion detection (4.6%) from η decays to $\gamma\gamma$, $\pi^+\pi^-\pi^0$, and $3\pi^0$; $\mathcal{R}$-r and π^0/η veto requirements (2.8%–5.5%) from $B^- \to D^0\pi^-$, $D^0 \to K^-\pi^+$ and $\bar{B}^0 \to D^+\pi^-$, $D^+ \to K^-\pi^+\pi^+$; the $\omega \to \pi^+\pi^-\pi^0$ branching fraction (0.8%); and uncertainty due to MC statistics (0.5%–0.7%).

We perform an unbinned extended maximum likelihood fit to candidates satisfying $|\Delta E| < 0.5$ GeV and $M_{\rm bc} > 5.2$ GeV/c^2, individually and simultaneously for the three signal modes. In the latter case we assume isospin symmetry, and we also simultaneously fit the two $\bar{B} \to \bar{K}^*\gamma$ modes. We describe the events in the fit region using a sum of functions for the signal, continuum, $K^*\gamma$ (for the three signal modes only), and other background hypotheses. The signal distribution is modeled as the product of a Crystal Ball line shape [12] in ΔE to reproduce the asymmetric ECL energy response, and a Gaussian (another Crystal Ball line shape) in $M_{\rm bc}$ for the mode without (with) a π^0 in the final state. The signal parameters for $M_{\rm bc}$ and ΔE are determined from separate fits to the $B^- \to K^{*-}\gamma$ and $\bar{B}^0 \to \bar{K}^{*0}\gamma$ samples for the modes with and without a neutral pion, respectively. The branching fraction is the only parameter that is allowed to float for the signal component. The continuum background component is modeled as the product of a linear function in ΔE and an ARGUS function [13] in $M_{\rm bc}$. The continuum shape parameters and normalizations are mode dependent and allowed to float. We use the distributions of MC events to model the shapes of other background components. The size of the $K^*\gamma$ background component in each signal mode is constrained using the fit to the $K^*\gamma$ events and the known misidentification probability. Other radiative and charmless decays are considered as an additional background component when we extract the signal yield. The levels of the other backgrounds are fixed using known branching fractions or upper limits [14]. We constrain branching fractions in the simultaneous fit using the isospin relations [4,15] $\mathcal{B}(\bar{B} \to (\rho,\omega)\gamma) \equiv \mathcal{B}(B^- \to \rho^-\gamma) = 2\frac{\tau_{B^+}}{\tau_{B^0}}\mathcal{B}(\bar{B}^0 \to \rho^0\gamma) = 2\frac{\tau_{B^+}}{\tau_{B^0}}\mathcal{B}(\bar{B}^0 \to \omega\gamma)$ and $\mathcal{B}(\bar{B} \to \bar{K}^*\gamma) \equiv \mathcal{B}(B^- \to K^{*-}\gamma) = \frac{\tau_{B^+}}{\tau_{B^0}}\mathcal{B}(\bar{B}^0 \to \bar{K}^{*0}\gamma)$, where $\frac{\tau_{B^+}}{\tau_{B^0}} = 1.076 \pm 0.008$ [14].

TABLE I. Yield, significance with (without) systematic uncertainty, efficiency, and branching fraction ($\mathcal{B}$) for each mode.

Mode	Yield	Significance	Efficiency (%)	$\mathcal{B}$ (10^{-6})
$B^- \to \rho^-\gamma$	8.5	1.6 (1.6)	3.86 ± 0.23	$0.55^{+0.42+0.09}_{-0.36-0.08}$
$\bar{B}^0 \to \rho^0\gamma$	20.7	5.2 (5.2)	4.30 ± 0.28	$1.25^{+0.37+0.07}_{-0.33-0.06}$
$\bar{B}^0 \to \omega\gamma$	5.7	2.3 (2.6)	2.61 ± 0.21	$0.56^{+0.34+0.05}_{-0.27-0.10}$
$\bar{B} \to (\rho,\omega)\gamma$	36.9	5.1 (5.4)	...	$1.32^{+0.34+0.10}_{-0.31-0.09}$

The results of the fits are shown in Fig. 2 and listed in Table I. The simultaneous fit gives

$$\mathcal{B}(\bar{B} \to (\rho,\omega)\gamma) = (1.32^{+0.34+0.10}_{-0.31-0.09}) \times 10^{-6}, \quad (1)$$

where the first and second errors are statistical and systematic, respectively. The result is consistent with previous results [2,3] and in agreement with SM predictions [4,5]. The significance of the simultaneous fit is 5.1σ, where the significance is defined as $\sqrt{-2\ln(\mathcal{L}_0/\mathcal{L}_{\rm max})}$, and $\mathcal{L}_{\rm max}$ ($\mathcal{L}_0$) is the value of the likelihood function when the signal branching fraction is floated (set to zero). Here, the like-

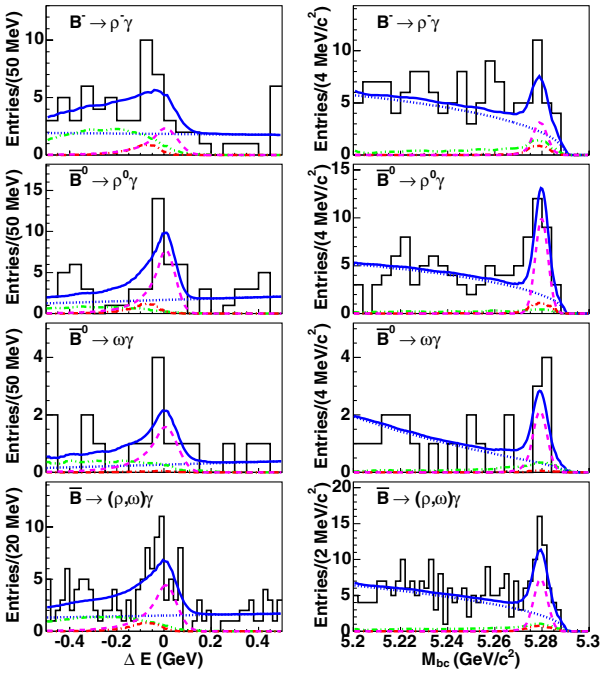

FIG. 2 (color online). Projections of the fit results to $M_{\rm bc}$ (in the region -0.10 GeV $< \Delta E < 0.08$ GeV) and ΔE (in the region 5.273 GeV/$c^2 < M_{\rm bc} < 5.285$ GeV/c^2) for the individual and simultaneous fits. Curves show the signal (dashed line), continuum (dotted line), $\bar{B} \to \bar{K}^*\gamma$ (dot-dashed line), other B decay background (dot-dot-dashed line) components, and the total fit result (solid line).

lihood function from the fit is convolved with a Gaussian systematic error function in order to include the systematic uncertainty. The invariant $\pi\pi(\pi)$ mass and helicity angle distributions for the events in the signal box are consistent with those expected from the sum of the signal and background components. The fit also gives $\mathcal{B}(\bar{B} \to \bar{K}^*\gamma) = (41.1^{+1.4}_{-1.3}) \times 10^{-6}$ (statistical error only), which is consistent with the world average value [14]. The individual fit results are in marginal agreement with the isospin relation. We test our fitting procedure using MC simulation and find no statistically significant bias. We perform MC pseudoexperiments where events are generated according to the isospin relation; from the two-dimensional distribution of the deviation between the B^- and averaged $\bar{B}^0$ rates and that between the $\rho^0\gamma$ and $\omega\gamma$ rates, we find the probability to observe an isospin violation equal to or larger than our measurement to be 4.9%. The expected level of isospin violation is within $\pm 10\%$ [4].

The systematic error is estimated by varying each of the fixed parameters by $\pm 1\sigma$ and then taking the quadratic sum of the deviations in the branching fraction from the nominal value. We note that the ARGUS background shape in the fit to the $\omega\gamma$ mode is steeper than those for the other two modes. Therefore we also vary the ARGUS shape parameter for the $\omega\gamma$ mode by -2σ and include the deviation in the systematic error.

The ratio $\mathcal{B}(\bar{B} \to (\rho, \omega)\gamma)/\mathcal{B}(\bar{B} \to \bar{K}^*\gamma) = 0.032 \pm 0.008(\text{stat}) \pm 0.002(\text{syst})$, which we obtain from a separate fit, can be used to determine $|V_{td}/V_{ts}|$. The fit takes into account the correlated systematic errors between the signal and $K^*\gamma$ modes and thus gives a reduced total error. Using the relation [16] $\frac{\mathcal{B}(\bar{B}\to(\rho,\omega)\gamma)}{\mathcal{B}(\bar{B}\to\bar{K}^*\gamma)} = |\frac{V_{td}}{V_{ts}}|^2 \frac{(1-m^2_{(\rho,\omega)}/m^2_B)^3}{(1-m^2_{K^*}/m^2_B)^3}\zeta^2[1 + \Delta R]$, where the form factor ratio $\zeta = 0.85 \pm 0.10$ and the $SU(3)$-breaking correction $\Delta R = 0.1 \pm 0.1$, we obtain

$$|V_{td}/V_{ts}| = 0.199^{+0.026}_{-0.025}(\text{exp})^{+0.018}_{-0.015}(\text{theor}). \quad (2)$$

We obtain a 95% confidence level interval of $0.142 < |V_{td}/V_{ts}| < 0.259$ using an ensemble of MC samples in which the experimental error is a quadratic sum of the asymmetric Gaussian statistical and systematic errors, and the theory error is a flat distribution in the given range. This result is in agreement with the range favored by a fit to the unitarity triangle [17] assuming $|V_{ts}| = |V_{cb}|$.

In conclusion, we observe the process $b \to d\gamma$ using the $B \to \rho\gamma$ and $\omega\gamma$ modes. The resulting branching fractions are consistent with SM predictions [4,5]. The ratio of the $\bar{B} \to (\rho, \omega)\gamma$ branching fraction to that for $\bar{B} \to \bar{K}^*\gamma$ is used to determine $|V_{td}/V_{ts}|$.

We thank the KEKB group for the excellent operation of the accelerator, the KEK cryogenics group for the efficient operation of the solenoid, and the KEK computer group and the NII for valuable computing and Super-SINET network support. We acknowledge support from MEXT and JSPS (Japan); ARC and DEST (Australia); NSFC (Contract No. 10175071, China); DST (India); the BK21 program of MOEHRD and the CHEP SRC program of KOSEF (Korea); KBN (Contract No. 2P03B 01324, Poland); MIST (Russia); MHEST (Slovenia); SNSF (Switzerland); NSC and MOE (Taiwan); and DOE (USA).

[1] M. Kobayashi and T. Maskawa, Prog. Theor. Phys. **49**, 652 (1973); N. Cabibbo, Phys. Rev. Lett. **10**, 531 (1963).
[2] D. Mohapatra *et al.* (Belle Collaboration), Phys. Rev. D **72**, 011101 (2005).
[3] B. Aubert *et al.* (*BABAR* Collaboration), Phys. Rev. Lett. **94**, 011801 (2005).
[4] A. Ali and A. Parkhomenko, Eur. Phys. J. C **23**, 89 (2002); C.-D. Lu, M. Matsumori, A. I. Sanda, and M.-Z. Yang, Phys. Rev. D **72**, 094005 (2005).
[5] In addition to Ref. [4], see, e.g., S. Bosch and G. Buchalla, Nucl. Phys. **B621**, 459 (2002); T. Huang, Z. Li, and H. Zhang, J. Phys. G **25**, 1179 (1999); R. Fleischer and S. Recksiegel, Phys. Rev. D **71**, 051501(R) (2005); M. Beneke, T. Feldmann, and D. Seidel, Eur. Phys. J. C **41**, 173 (2005).
[6] For example, A. Arhrib, C.-K. Chua, and W.-S. Hou, Eur. Phys. J. C **21**, 567 (2001); A. Ali and E. Lunghi, Eur. Phys. J. C **26**, 195 (2002); Z.-J. Xiao and C. Zhuang, Eur. Phys. J. C **33**, 349 (2004).
[7] S. Kurokawa and E. Kikutani, Nucl. Instrum. Methods Phys. Res., Sect. A **499**, 1 (2003).
[8] A. Abashian *et al.* (Belle Collaboration), Nucl. Instrum. Methods Phys. Res., Sect. A **479**, 117 (2002).
[9] S. H. Lee *et al.* (Belle Collaboration), Phys. Rev. Lett. **91**, 261801 (2003).
[10] G. C. Fox and S. Wolfram, Phys. Rev. Lett. **41**, 1581 (1978).
[11] H. Kakuno *et al.*, Nucl. Instrum. Methods Phys. Res., Sect. A **533**, 516 (2004). We find that the use of r increases the signal efficiency by 5% to 50% for the same background level.
[12] J. E. Gaiser *et al.* (Crystal Ball Collaboration), Phys. Rev. D **34**, 711 (1986).
[13] H. Albrecht *et al.* (ARGUS Collaboration), Phys. Lett. B **241**, 278 (1990).
[14] Heavy Flavor Averaging Group, winter 2005 results, http://www.slac.stanford.edu/xorg/hfag/.
[15] A. Ali, V. M. Braun, and H. Simma, Z. Phys. C **63**, 437 (1994).
[16] A. Ali, E. Lunghi, and A. Parkhomenko, Phys. Lett. B **595**, 323 (2004).
[17] S. Eidelman *et al.*, Phys. Lett. B **592**, 1 (2004).